



Original Research Article

Influence of temperature on energy band gap and other properties of undoped and cadmium doped manganese sulphide (MnS:Cd) synthesized for photovoltaic and optoelectronic application

Imosobomeh L. Ikhioya^{a,*} , Ijeh Rufus^b, Nwamaka Ifeyinwa Akpu^c 

^a Department of Physics and Astronomy, Faculty of Physical Sciences, University of Nigeria, Nsukka, Enugu State

^b Department of Physics, University of Delta, Agbor, Delta State, Nigeria

^c Department of Physics, Michael Okpara University of Agriculture, Umudike, Umuahia, Abia State, Nigeria

ARTICLE INFORMATION

Received: 24 January 2022

Received in revised: 19 February 2022

Accepted: 2 March 2022

Available online: 18 March 2022

DOI: [10.48309/JMNC.2022.2.1](https://doi.org/10.48309/JMNC.2022.2.1)

KEYWORDS

Electrochemical deposition

Cadmium doped manganese sulphide

Structural features

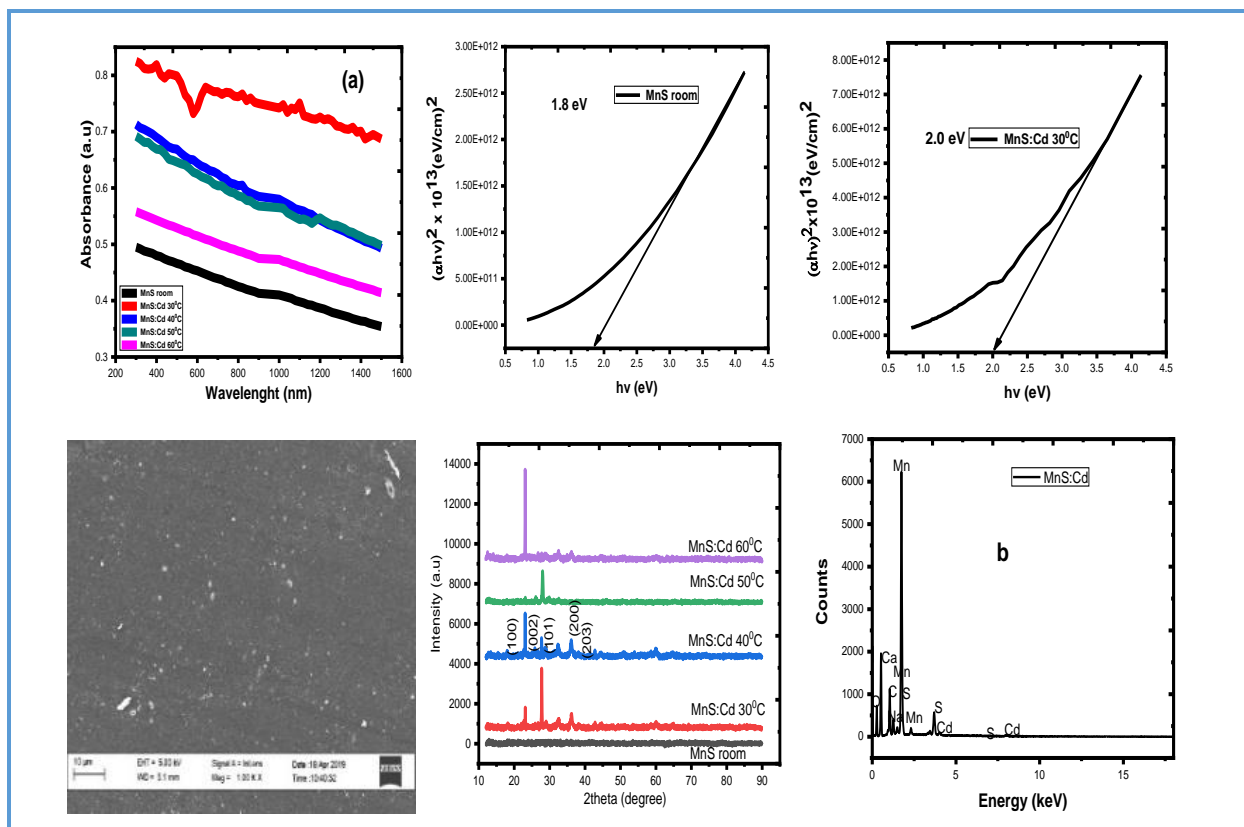
Band gap energy

Photovoltaic

ABSTRACT

The synthesis of undoped and cadmium doped Manganese Sulphide (MnS:Cd) films consists of; Manganese (ii) acetate tetrahydrate ($C_4H_6MnO_4 \cdot 4H_2O$), cadmium sulphate ($CdSO_4$), and Thiourea $SC(NH_2)_2$. The electrochemical deposition (ECD) method was adopted in this research. The samples' morphological, structural, elemental, optical, and thickness were studied using appropriate techniques. The films exhibited uniform distribution of spherical balls from the morphological studies while the structural features showed crystalline peaks at (100), (002), (101, (200)) and (203) planes at 2θ (22.66, 27.77, 32.44, 36.25 and 42.80) angles. The elemental composition analysis of the deposited samples confirmed the elements deposited in the samples. For optical studies, we observed enhanced characteristics upon doping. The absorbance, transmittance, and reflectance increase as the incident radiation wavelength increases with an increase in bandgap energy from 1.8 eV – 3.6 eV. The synthesized films find potential application in photovoltaic and optoelectronics. The material thickness obtained was seen to vary directly proportionally with the energy band gap values. More so, the addition of Cd to pure MnS and increase in deposition temperature for MnS:Cd increased the thickness of the material.

Graphical Abstract



Introduction

Manganese (Mn) is a transition metal with unique physical and chemical properties. It has photovoltaic and optoelectronic applications [1–3]. Metal sulphide can be deposited on glass, polymer, or metal substrates immersed in solutions containing metal complex ions and a sulphide source [2]. Manganese sulphide (MnS) is a fascinating material for both fundamental and applied research, particularly when its bulk properties are modulated by shrinking to the nanosize (<100 nm). MnS has various applications in photovoltaic, solar cell fabrication, and the electronic industries [1]. More so, cadmium doped Manganese Sulphide thin-films have piqued the interest of researchers due to their novel magnetic and magneto-optical properties derived from hybridization among the 3d Mn and CdS Sp-

hexagonal. The introduction of a large mole fraction shifts the intrinsic edge into the visible region, dominating the optical properties [4]. Many researchers have worked on CdMnS material via electrochemical deposition technique [5–7], vacuum evaporation [8], CBD [9–13], sputtering, and spray pyrolysis [14, 15]. The ECD technique was used to grow CdMnS material for photovoltaic application. Among the different techniques, the electrochemical deposition method gives an easy way of depositing films for photovoltaic and solar applications because of its economic, simplicity, and laboratory setup. Besides, the electrochemical deposition method could be used for the large-scale fabrication of material for commercial purposes.

In this research, we report the influence of temperature on the energy band gap and other properties of undoped and cadmium-doped

manganese sulphide (MnS: Cd) synthesized via electrochemical deposition method for photovoltaic and optoelectronic application.

Experimental

Materials and methods

The chemicals used for the synthesis were analytically graded. They include manganese (ii) acetate tetrahydrate ($C_4H_6MnO_4 \cdot 4H_2O$), Cadmium sulphate ($CdSO_4$), and Thiourea $SC(NH_2)_2$. The electrochemical deposition (ECD) method involves deposition any substance on an electrode surface during electrolysis. Enclosed in the electrochemical bath are deionized water, a cationic source (i.e. $C_4H_6MnO_4 \cdot 4H_2O$, $CdSO_4$ for Mn^{2+} , Cd^{2+}), and an anionic source ($SC(NH_2)_2$ for S^{2-}).

Procedure for the synthesis of undoped and MnS doped Cd materials

The synthesis of undoped and MnS doped Cd materials was done using an aqueous solution of 0.1 mol solution of $C_4H_6MnO_4 \cdot 4H_2O$ and $SC(NH_2)_2$ as sources of Mn^{2+} ion (as a cation) and S^{2-} ion (as an anion) respectively. In comparison, 0.1 mol solution of $CdSO_4$ serves as the dopant (Cd^{2+} ion).

The electrochemical deposition technique was adopted in depositing the films. The electrochemical setup consisted of a bath consisting of 20 mL each of the cationic precursor, anionic precursor, and distilled water in a 100 mL beaker. The cubicle subsists

three-electrode configurations; platinum mesh as the positive, a silver-silver chloride electrode (Ag/AgCl) as the reference electrode, and a working electrode/negative. The fluorine-doped tin oxide slide was placed perpendicular to the cubicle, all-inclusive the counter and reference electrodes for all deposition. The synthesis was carried out under a Potentiostat condition of -200 mV versus SCE for 10 s. The synthesized films were therefore cleaned and dried. In the deposition, the target materials were measured into the beakers, which exist of equal volumes (20 mL) of $C_4H_6MnO_4 \cdot 4H_2O$, selenium, and 10 mL of $CdSO_4$ solutions. The V supply was kept at 10 V. After the syntheses, the films were annealed and heated for 30 min to eliminate centralized stresses. The cadmium dopant was introduced by adding 10 mL of 0.1 mol of $CdSO_4$ into the electrochemical bath. The undoped sample was obtained at room temperature (26 °C), while the Cd doped MnS samples were obtained at various temperatures (30 – 60 °C) at pH values of 7.2, Table 1 summarizes the deposition parameters of MnS and MnS: Cd at varied temperatures. The MnS and MnS doped Cd films deposited were characterized in other to ascertain their morphological, structural, elemental, optical, and electrical properties using Scanning Electron Microscopy, Advance BrukerD8 X-ray diffractometer with Cu $K\alpha$ line ($\lambda = 1.54056$ Å) in 2θ range from 10° – 90° , EDX, UV-1800 Visible Spectrophotometer, and four-point probe respectively.

Table 1. Summary of deposition parameters of MnS and MnS: Cd at varied temperature

Sample	$CdSO_4$ (mL)	$C_4H_6MnO_4 \cdot 4H_2O$ (mL)	$SC(NH_2)_2$ (mL)	Temperature (Degree)	Time (Sec)	Voltage (V)
MnS room	-	20	20	Room	10	10
MnS: Cd 30 °C	10	20	20	30	10	10
MnS: Cd 40 °C	10	20	20	40	10	10
MnS: Cd 50 °C	10	20	20	50	10	10
MnS: Cd 60 °C	10	20	20	60	10	10

Results and Discussion

The structural study of undoped and MnS:Cd materials at different temperatures

Figure 1 displays the XRD pattern of the undoped and MnS:Cd materials grown on Fluorine doped tin oxide substrates at different temperatures. The samples exhibit a polycrystalline hexagonal structure with visible crystalline peaks at (100), (002), (101), (200), and (203) planes at 2θ (22.66, 27.77, 32.44, 36.25, and 42.80) diffraction angles respectively with JCPDS card no. 07-2206 for MnS and 07-3049 for MnS:Cd (Table 2) [16–18].

Surface micrograph analysis of undoped and MnS:Cd materials at different temperatures

The surface morphology of undoped and MnS:Cd thin materials at different temperatures is shown demonstrated in Figure 2. For MnS deposited at room temperature, the result reveals round tiny circular nanoparticles. In contrast, for MnS:Cd at 30 °C and MnS:Cd at 40 °C, the nanoparticles were well packed as a result of the company of chargeless energy properties of cramped particles. For MnS:Cd at 50 °C and MnS:Cd at 60 °C, the nanoparticles become more homogenous with no cracks on the surface [19].

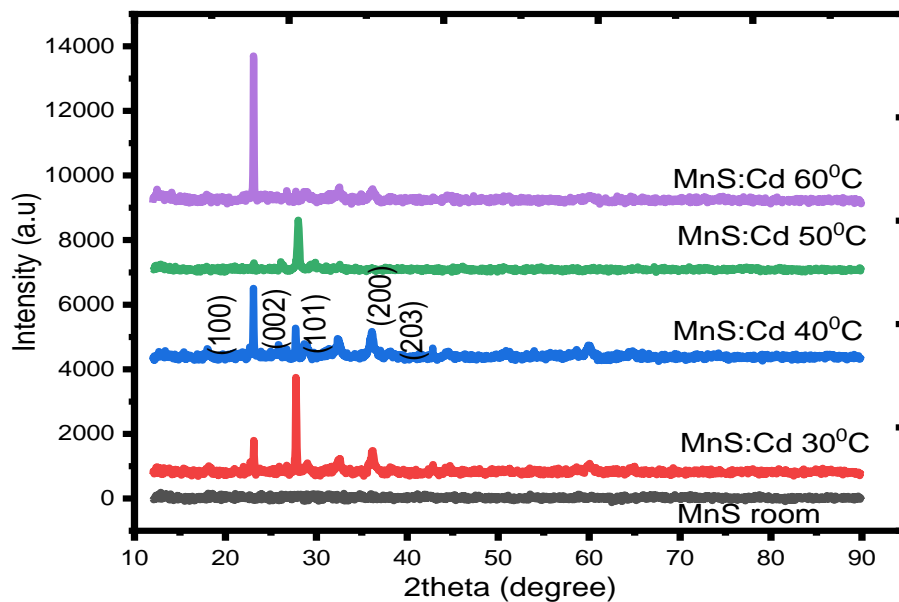


Figure 1. XRD pattern of undoped and MnS:Cd materials at different temperatures

Table 2. Obtained structural values for MnS and MnS:Cd materials at different temperatures

Sample	2θ (degree)	(hkl)	d-spacing Å	a (Å)	FWHM (β)	Crystallite Size, D (nm)
MnS	22.66	100	3.91	6.78	0.18	0.76
MnS:Cd30 °C	27.77	002	3.20	6.41	0.20	0.68
MnS:Cd 40 °C	32.44	101	2.75	5.51	0.14	0.97
MnS:Cd 50 °C	36.25	200	2.47	5.53	0.22	0.64
MnS:Cd 60 °C	42.80	203	2.11	5.17	0.22	0.66

Elemental analysis of undoped and MnS:Cd materials at different temperatures

Figure 3 reveals the EDX spectra of the MnS and MnS:Cd samples. The spectra confirmed basic elemental constituents of the film: Mn, Se, Cd on the substrate surfaces. The undoped

sample has its elemental constituents displayed in Figure 3a, while the doped samples at varying concentrations exhibited similar elemental compositions and are singly represented in Figure 3b. Other elements on the spectrum might result from the conducting FTO glass slide used as substrate.

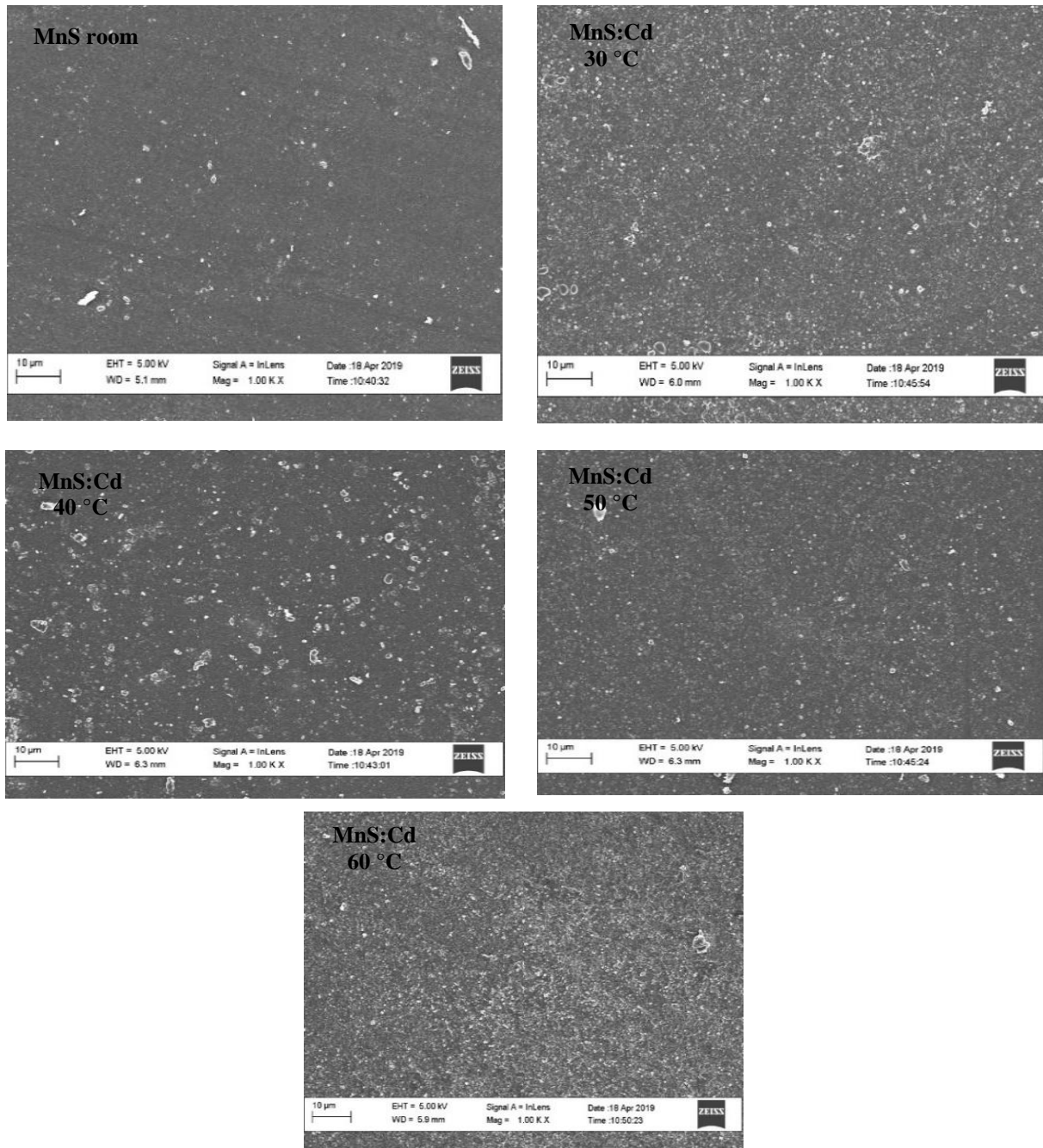


Figure 2. Surface morphology of undoped and MnS:Cd materials at different temperatures

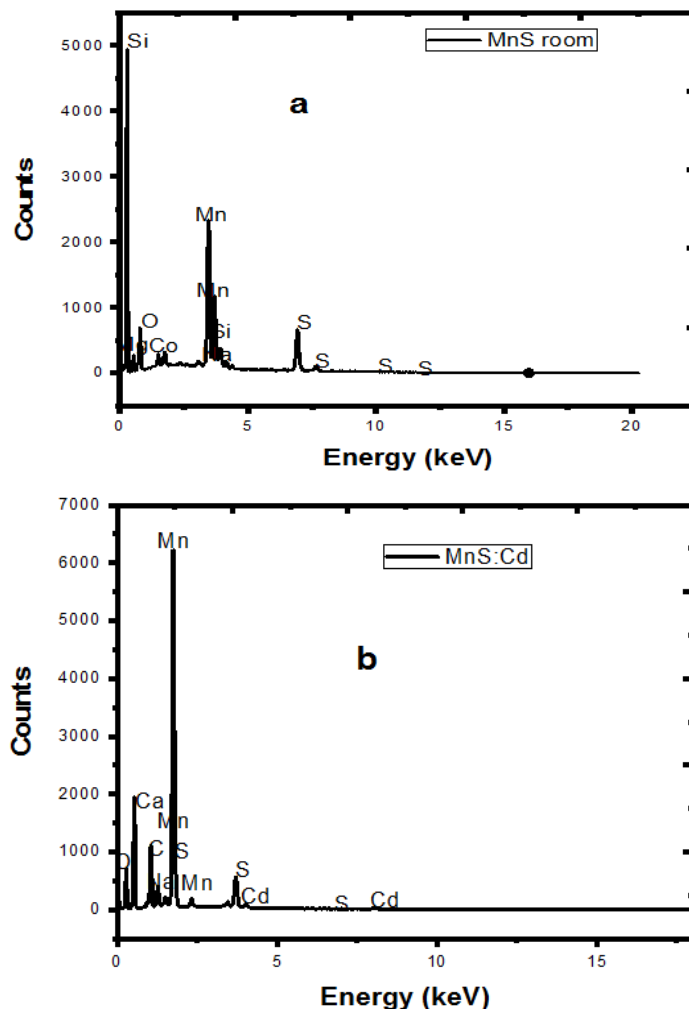


Figure 3. EDX Spectra of undoped and MnS:Cd materials at different temperatures

The optical study of undoped and MnS:Cd materials at different temperatures

The absorbance spectra of undoped and MnS:Cd materials at different temperatures are shown in [Figure 4a](#). The graph reveals a decrease in the absorbance value of the samples as the wavelength of the electromagnetic radiation spectra increases. It was noticed that the grown films at 40 °C and 50 °C follow the same trend and recorded absorbance values of 0.73 and 0.69, respectively. This result is in line with the reports from Munde and Ravangave, Gumus et al., and Tepparo *et al.* [11-13]. The sample MnS:Cd at 30 °C recorded the highest absorbance values of 0.89, while the one grown

with the highest temperature at 60 °C recorded the lowest absorbance of 0.56 (for all Cd doped samples). The manganese sulphide sample MnS deposited at room temperature shows the lowest absorbance value in the spectra, which implies that doping with cadmium enhances the absorbance of MnS thin films, thereby making them good material for photovoltaic application.

The transmittance spectra of spectra of undoped and MnS:Cd materials at different temperatures are shown in [Figure 4b](#). An increase in the electromagnetic radiation wavelength resulted in an increase in transmittance value for samples MnS, MnS:Cd at

30 °C, and MnS:Cd at 50 °C and a decrease for sample MnS:Cd at 40 °C and MnS:Cd at 60 °C. It was observed that sample MnS:Cd at 40 °C and MnS:Cd at 60 °C have the plot's highest transmittance spectra. The sample MnS:Cd at 30 °C recorded the lowest transmittance while the one grown at the highest temperature at 60 °C recorded the transmittance value of 0.64% which shows that the deposition temperature increases the transmittance of MnS:Cd increases and decreases in some cases reported by [16]. The manganese sulphide sample MnS deposited at room temperature transmit above 0.25% in the spectra, which shows that doping with cadmium enhances the transmittance of MnS thin films.

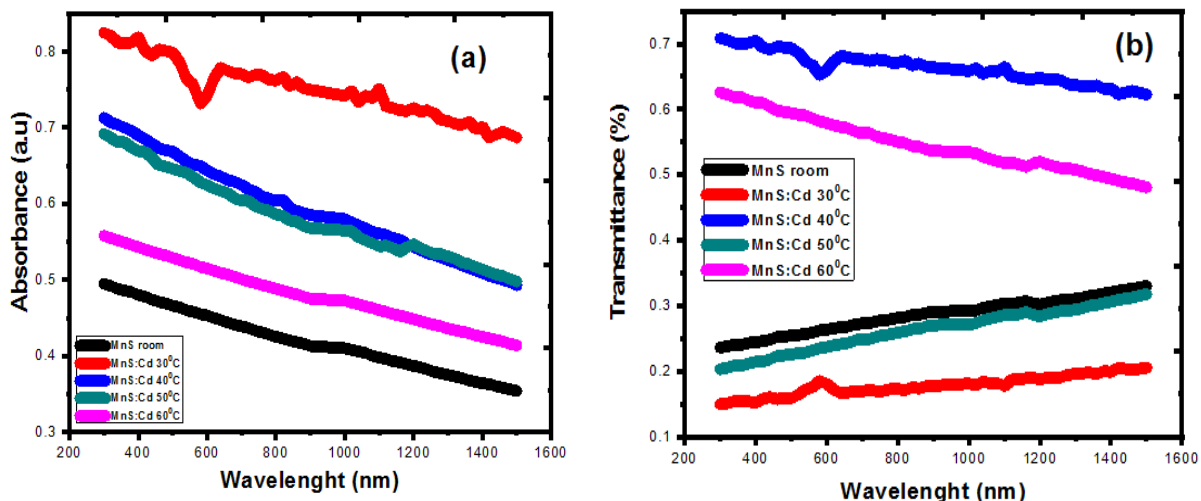
The reflectance spectra of undoped and MnS:Cd materials at different temperatures are shown in Figure 4c. The reflectance graph in Figure 4c depicts that the reflectance value increases for sample MnS, MnS:Cd at 30 °C, MnS:Cd at 50 °C, MnS:Cd at 60 °C, and decreases for sample MnS:Cd at 40 °C as the wavelength of the electromagnetic radiation of the incident photon increases. It was observed that sample MnS:Cd at 40 °C has the highest reflectance spectra in the plot. The sample MnS:Cd at 30 °C recorded the lowest reflectance. The sample grown at the highest temperature (60 °C)

recorded a reflectance value of 0.189%. In summary, variation in deposition temperature affected the reflectance value of MnS:Cd. The manganese sulphide sample MnS deposited at room temperature reflected above 0.149% in the spectra, which shows that doping with cadmium enhances the reflectance of MnS thin.

The energy bandgap of the samples was evaluated using Equation 1. Figure 5a-d shows the plot of αhv against hv for undoped and MnS:Cd films grown at various temperatures and extrapolating the linear part of the graph down to the horizontal at $\alpha hv = 0$ gives the energy bandgap of the different samples [20].

$$\alpha hv = A(hv - E_g)^n \quad (1)$$

The introduction of Cd dopant was observed to widen the energy band gap of pure MnS from 1.8 to 3.6 eV making it a good material for power electronics and optoelectronics. The energy band gap values of undoped and Cd doped MnS with their corresponding thickness results are outlined in Table 3. These values were observed to vary directly proportionally to each other. More so, the addition of Cd to pure MnS and increase in deposition temperature for MnS: Cd increased the thickness of the material. A similar result was reported by Akpu *et al.* [21].



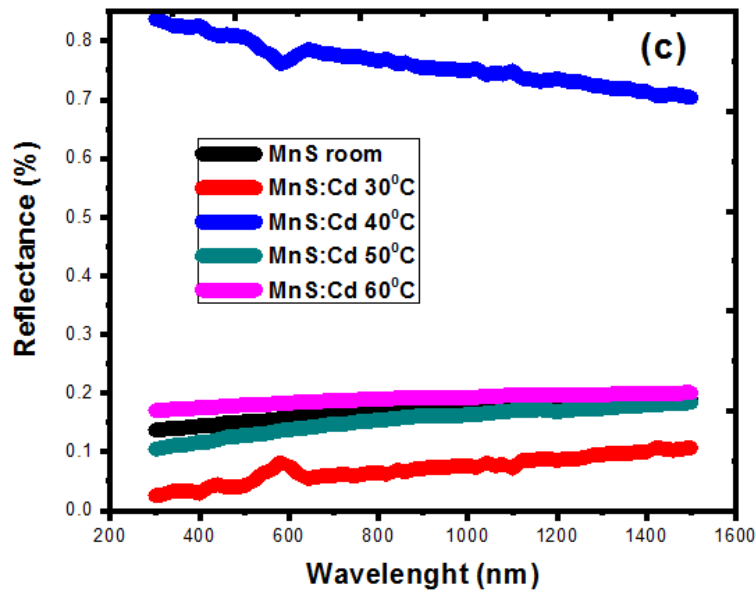
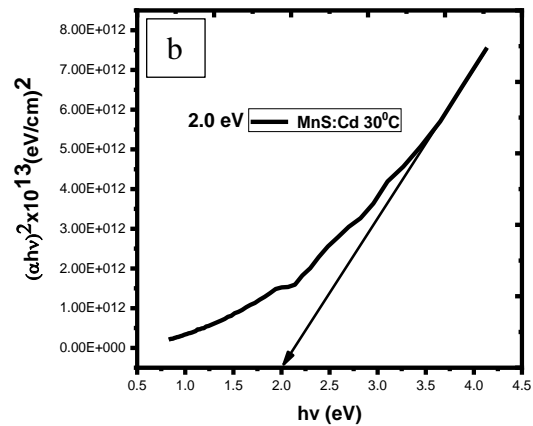
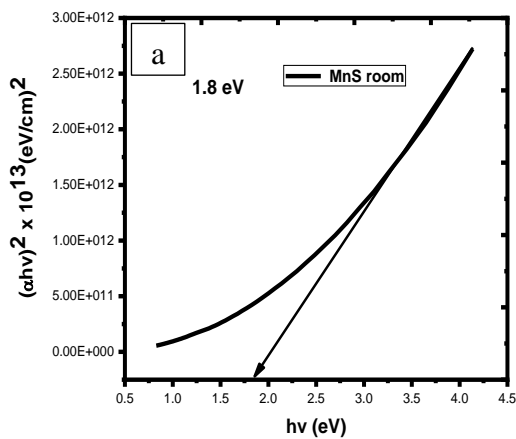


Figure 4. Absorbance a), transmittance b), and reflectance c) against wavelength for undoped and MnS:Cd materials at different temperatures

Table 3. Bandgap Energy and thickness of MnS and MnS:Cd thin materials at different deposition temperatures

Samples	Thickness (nm)	E_g (eV)
MnS	122.11	1.8
MnS: Cd 30 °C	127.52	2.0
MnS: Cd 40 °C	132.61	3.0
MnS: Cd 50 °C	135.42	3.4
MnS: Cd 60 °C	138.71	3.6



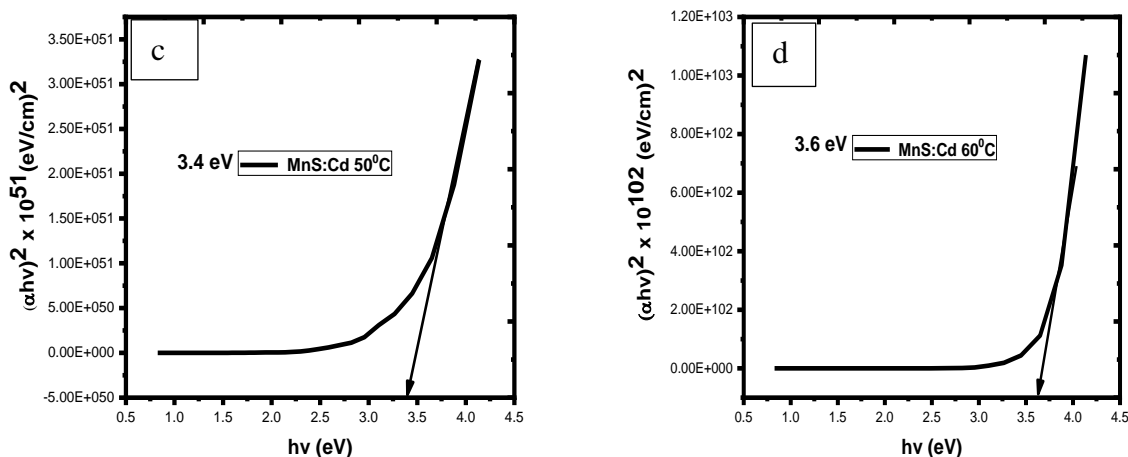


Figure 5. Plot of absorption coefficient squared versus photon energy for undoped and MnS:Cd at different deposition temperatures

Conclusions

The study of the influence of temperature on the energy band gap and other properties of undoped and cadmium doped manganese sulphide (MnS:Cd) synthesized via electrochemical deposition method and characterized for photovoltaic and optoelectronic application has been successfully carried out. The morphological, structural, elemental, optical, and thickness of the samples were studied using scanning electron microscopy, x-ray diffractometry (XRD), Energy dispersive x-ray spectroscopy (EDX), UV-visible spectrophotometer (UV-vis), and four-point probe technique, respectively. The films exhibited uniform distribution of spherical balls from the morphological studies while the structural features showed crystalline peaks at (100), (002), (101, (200)) and (203) planes at 2θ (22.66, 27.77, 32.44, 36.25 and 42.80) angles. The elemental composition analysis of the deposited samples confirmed the elements deposited in the samples. For optical studies, we observed enhanced characteristics upon doping. Most of the samples' absorbance,

transmittance, and reflectance values increase as the wavelength of incident radiation increases. Energy bandgap ranging from 1.8 eV –3.6 eV was obtained. The introduction of Cd dopant was observed to widen the energy band gap of pure MnS from 1.8 to 2.0 eV. At the same time, an increase in deposition temperature was seen to widen it more up to 3.6eV, making it a good material for power electronics and optoelectronics. The material thickness obtained using four-point probes varies directly proportionally with the energy band gap values. More so, the addition of Cd to pure MnS and increase in deposition temperature for MnS:Cd increased the thickness of the material.

Acknowledgments

We graciously acknowledge all the authors for their contribution to the success of the research.

Disclosure Statement

No potential conflict of interest was reported by the authors.

Orcid

Imosobomeh L. Ikhioya  0000-0002-5959-4427

Nwamaka Ifeyinwa Akpu  0000-0001-8062-9279

References

- [1]. Ikhioya I.L., Ugbo F.C., Ijabor B.O. *International Journal for Research in Applied and Natural Science*, 2018, **4**:1 [[Publisher](#)]
- [2]. Kassim A., Wee TeeT., Soon Min H., Abdullah A.H., Haziq Jusoh A., Nagalingam S. *Kasetsart Journal (Natural Science)*, 2010, **44**:446 [[Google Scholar](#)], [[Publisher](#)]
- [3]. Kassim A., Soon Min H. *International Journal of Chemistry Research*, 2010, **1**:1 [[Google Scholar](#)], [[Publisher](#)]
- [4]. Chaki S. H., Chauhan S. M., Tailor J. P., Deshpande M.P. *J Mater Res Technol.*, 2017, **6**:123 [[Crossref](#)], [[Google Scholar](#)], [[Publisher](#)]
- [5]. Ikhioya I.L., Ezeorba M.C., Okoroh D.O., Rand A.C., Obasi C.O. *SSRG International Journal of Applied Physics (SSRG-IJAP)*, 2020, **7**:102 [[Crossref](#)], [[Google Scholar](#)], [[Publisher](#)]
- [6]. Ikhioya I.L. Ekpunobi A.J. *Journal of Nigeria Association of Mathematical Physics*, 2015, **29**:325 [[Google Scholar](#)], [[Publisher](#)]
- [7]. Ikhioya I.L., Okoli D.N., Ekpunobi A.J. *Asian Journal of Nanoscience and Materials*, 2020, **3**:189 [[Crossref](#)], [[Google Scholar](#)], [[Publisher](#)]
- [8]. Iacomi F., Salaoru I., Apetroaei N., Vasile A., Teodorescu C.M., Macovei D. *Journal of Optoelectronics and Advanced Materials*, 2006, **8**:266 [[Google Scholar](#)]
- [9]. Sadoon A., Sharma R. *International Journal of Pure and Applied Physics.*, 2017, **13**:241 [[Google Scholar](#)], [[Publisher](#)]
- [10]. Fan D.B., Wang H., Zhang Y.C., Cheng J., Wang B., Yan H. *Mater Chem Phys.*, 2003, **80**:44 [[Crossref](#)], [[Google Scholar](#)], [[Publisher](#)]
- [11]. Tepparo R., D'Arco P., Lichanota A. *Chem Phys Lett.*, 1997, **273**:83 [[Crossref](#)], [[Google Scholar](#)], [[Publisher](#)]
- [12]. Chaki S.H., Deshpande M.P., Tailor J.P., Mahato K.S., Chaudhary M.D. *Adv Mater Res.*, 2012, **584**:243 [[Crossref](#)], [[Google Scholar](#)], [[Publisher](#)]
- [13]. Gumus C., Ulutas C., Esen R., Ozkendir O.M., Ufuktepe Y. *Thin Solid Films*, 2005, **492**:1 [[Crossref](#)], [[Google Scholar](#)], [[Publisher](#)]
- [14]. Chowdhuri M.R.I., Podder J., Isla A.B.M.O. *Cryst Res Technol*, 2011, **46**:267 [[Crossref](#)], [[Google Scholar](#)], [[Publisher](#)]
- [15]. Agbim E.G., Ikhioya I.L., Ekpunobi A.J. *Asian Journal of Nanoscience and Materials*, 2020, **3**:47 [[Crossref](#)], [[Publisher](#)]
- [16]. Ogunsola O.E., Oladiran E.O. *Journal of Nigeria Association of Mathematical Physics*, 2014, **28**:281 [[Google Scholar](#)], [[Publisher](#)]
- [17]. Riha S.C., Koegel A.A., Meng X., Kim I.S., Cao Y., Pellin M.J., Elam J.W., Martinson A.B.F. *ACS Appl. Mater. Interfaces*, 2016, **8**:2774 [[Crossref](#)], [[Google Scholar](#)], [[Publisher](#)]
- [18]. Zuo F., Zhang B., Tang X., Xie Y. *Nanotechnology*, 2007, **18**:215608 [[Crossref](#)], [[Google Scholar](#)], [[Publisher](#)]
- [19]. Akpu N.I., Asiegbe A.D., Nnanna L.A., Ikhioya I.L. Mgbeojedo T.I. *J Mater Sci: Mater Electron*, 2021, **33**:1154 [[Crossref](#)], [[Google Scholar](#)], [[Publisher](#)]
- [20]. Akpu N.I., Asiegbe A.D., Nnanna L.A., Ikhioya I.L., Mgbeojedo T.I. *Arabian Journal for Science and Engineering*, 2022 [[Crossref](#)], [[Google Scholar](#)], [[Publisher](#)]

How to cite this manuscript: Imosobomeh L. Ikhioya*, Ijeh Rufus, Nwamaka Ifeyinwa Akpu. Influence of temperature on energy band gap and other properties of undoped and cadmium doped manganese sulphide (MnS: Cd) synthesized for photovoltaic and optoelectronic application. *Journal of Medicinal and Nanomaterials Chemistry*, 4(2) 2022, 88-97. DOI: [10.48309/JMNC.2022.2.1](https://doi.org/10.48309/JMNC.2022.2.1)